University of Nebraska - Lincoln
DigitalCommons@University of Nebraska - Lincoln

Ralph Skomski Publications | Research Papers in Physics and Astronomy

June 1993

Nitrogen diffusion in Sm_2Fe_{17} and local elastic and magnetic properties

Ralph Skomski
University of Nebraska-Lincoln, rskomski2@unl.edu

J.M.D. Coey
Trinity College, Dublin, Ireland

Follow this and additional works at: https://digitalcommons.unl.edu/physicsskomski

Part of the Physics Commons

Skomski, Ralph and Coey, J.M.D., "Nitrogen diffusion in Sm_2Fe_{17} and local elastic and magnetic properties" (1993). *Ralph Skomski Publications*. 38.
https://digitalcommons.unl.edu/physicsskomski/38

This Article is brought to you for free and open access by the Research Papers in Physics and Astronomy at DigitalCommons@University of Nebraska - Lincoln. It has been accepted for inclusion in Ralph Skomski Publications by an authorized administrator of DigitalCommons@University of Nebraska - Lincoln.

Nitrogen diffusion in Sm_2Fe_{17} and local elastic and magnetic properties

R. Skomski and J. M. D. Coey
Department of Pure and Applied Physics, Trinity College, Dublin 2, Ireland

(Received 27 January 1992; accepted for publication 3 February 1993)

The reaction between nitrogen gas and an intermetallic compound is studied, with particular reference to Sm_2Fe_{17}, treating the $Sm_2Fe_{17}N_y$ system as a gas-solid solution. A simple lattice gas model is used to describe the reaction of nitrogen atoms with the metal lattice in terms of the net reaction energy $U_0 = -57 \pm 5$ kJ/mol. The equilibrium nitrogen concentration is calculated as a function of nitrogenation temperature and gas pressure. Refined diffusion parameters $D_0 = 1.02$ mm^2/s and $E_a = 133$ kJ/mol, determined by thermopiezic analysis of the initial stage of nitrogen absorption, are used to calculate nitrogen profiles and the time dependence of the mean nitrogen content during nitrogenation. Assuming mechanically isotropic grains the elastic strain and stress profiles are calculated. Main results are a large uniaxial strain near the surface of nonuniformly nitrided particles, and core expansion even in the absence of any nitrogen there. Curie temperature and K_1 profiles are calculated and suggestions are made regarding the influence of stress on coercivity and disproportionation of the material.

I. INTRODUCTION

Interest in the behavior of nitrogen in rare-earth intermetallics was sparked by the discovery that the magnetic properties of R_2Fe_{17} compounds are dramatically altered on nitrogen absorption.[1] The interstitial nitride $Sm_2Fe_{17}N_3$ is a promising new permanent magnet material, and extensive studies of the structure, intrinsic magnetic properties, hysteresis, and electronic structure of 2:17 nitrides have been published.[1–7] Gas-phase nitrogenation has been extended to other structural families of rare-earth intermetallics, and there are some summaries of the intermetallic nitride literature.[8]

Nitrogen typically occupies octahedral interstitial sites in these compounds, coordinated by two rare-earth and four iron atoms. In Sm_2Fe_{17}, the interstitial is the 9*e* site shown in Fig. 1, and the ideal composition is $Sm_2Fe_{17}N_3$. The nitride has the same crystal symmetry as the parent compound (space group $R\bar{3}m$), but the unit-cell volume is expanded by 6%. The nitrogen occupancy in $Sm_2Fe_{17}N_3$ was initially inferred from Sm—N bond lengths deduced from Sm L_{III} edge extended x-ray-absorption fine-structure (EXAFS) data,[2,3] but precise powder-neutron-diffraction studies on isostructural $Pr_2Fe_{17}N_3$ and $Nd_2Fe_{17}N_3$ have established that nitrogen occupies the 9*e* sites exclusively.[9] Usually, the 9*e* sites are not fully occupied, hence the practice of writing the formula as $Sm_2Fe_{17}N_{3-\delta}$. However, *nonequilibrium* methods such as ion implantation or use of flowing ammonia may populate other sites and yield nitrogen contents slightly larger than 3.

A key question discussed in Sec. II is whether the quasiequilibrium nitride is a simple gas-solid solution with a continuous range of intermediate nitrogen contents or a two-phase mixture of nitrogen-poor (α) and nitrogen-rich (β) phases.

Gas-phase nitrogenation is typically conducted at 400–500 °C on a finely ground R_2Fe_{17} powder in a pressure of about 1 bar N_2, or nitrogen-containing gas such as NH_3. Diffusion kinetics are sluggish at these temperatures, but if the temperature is increased a competing disproportionation reaction of the $Sm_2Fe_{17}N_3$ intervenes, as iron diffusion becomes significant.

In a previous diffusion study, the uptake of nitrogen by Sm_2Fe_{17} powders was examined at various temperatures as a function of time in the thermopiezic analyzer.[2] Data in the range 300–550 °C were fitted to the Arrhenius equation

$$D = D_0 e^{-E_a/kT}, \tag{1}$$

assuming a distribution of spherical particles of different sizes, which was determined by direct observation in the scanning electron microscope.[2] Results were $D_0 = 1.95 \times 10^{-4}$ mm^2/s and $E_a = 78$ kJ/mol. While the activation energy falls in the range observed for nitrogen in metals, the value of the prefactor is physically unreasonable. D_0 should be of order $a^2\nu_0$ where a is the jump distance in the diffusion process, and ν_0 is an attempt frequency.[10,11] The estimation $a \sim 3$ Å and $\nu_0 \sim 10^{13}$ s^{-1} yields $D_0 \sim 1$ mm^2/s.

During nitrogenation the inhomogeneous nitrogen distribution causes mechanical stress which must influence the properties of the material. It has been established that the increase of magnetization and Curie temperatures compared to pure Sm_2Fe_{17} are due to changes in the electronic structure which in turn are mainly a result of the lattice expansion.[1,12] Hence, the incompletely nitrided particles are expected to have an inhomogeneous T_c profile. On the other hand, elastic stress may intensify the decomposition of the material.

In the present work, we first examine the equilibrium nitrogen concentrations that may be expected in Sm_2Fe_{17} under various conditions. In Sec. IV we present data on the initial stages of nitrogen diffusion which yield a more plausible value of D_0; E_a and D_0 are then used to calculate diffusion lengths and nitrogen profiles for spherical particles under various nitrogenation conditions. The corresponding stress and strain profiles are then calculated in Sec. V. The effects of inhomogeneous nitrogen and strain profiles on magnetic properties are discussed in Sec. VI and conclusions are drawn in Sec. VII.

 0021-8979/93/117602-10$06.00 © 1993 American Institute of Physics

Downloaded 23 Mar 2007 to 129.93.16.206. Redistribution subject to AIP license or copyright, see http://jap.aip.org/jap/copyright.jsp

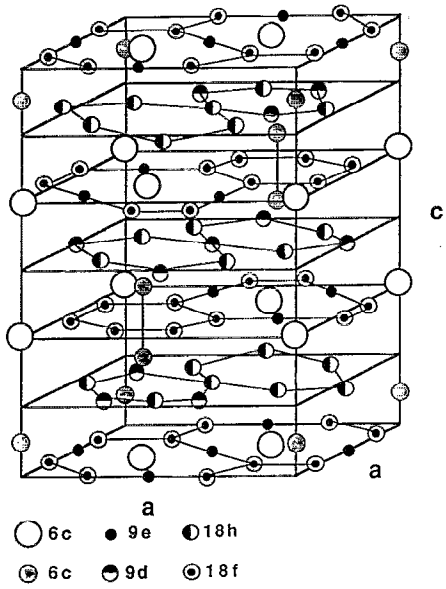

FIG. 1. Crystal structure of $Sm_2Fe_{17}N_3$. Sm occupies 6*c* sites, N occupies 9*e* sites, and the others are occupied by Fe.

II. EXPERIMENTAL METHODS

The experiments are done using hand-ground Sm_2Fe_{17} powder. In order to obtain an approximately monodisperse fraction the powder was sieved several times through 30 and 35 μm sieves.[13] The volume/surface ratio V_p/A_p of the powder was determined as 5.8 μm using light microscopy.

The diffusion reaction proceeds very slowly at temperatures below 500 °C, whereas above 600 °C a competing disproportionation reaction occurs.[1,2] To extend the accessible range of temperature, short-time thermopiezic analysis (TPA) measurements were used to determine the diffusion parameters. This method examines the initial stage of nitrogenation only, which reduces the measuring time necessary at low temperatures and avoids extensive disproportionation during the measurements at high temperatures. Additionally, as explained in Sec. IV, these results are independent of particle shape.

The measuring times vary between 30 s and 16 min. Gas expansion during the short time needed to reach an isothermal condition and a possible surface activation step lead to initial deviations from a square-root law whereas especially at higher temperatures the onset of the long-time disproportionation behavior restricts the possible measurement times. Only samples with less than 10% α-iron after the measurement have been included in the determination of the diffusion parameters, so the effects of the disproportionation reaction can be neglected.

To determine the net reaction energy U_0, long-time isothermal absorption experiments in the thermopiezic analyzer have been used.[14,15] The samples are heated in a closed nitrogen-containing chamber, and from the pressure change the nitrogen concentration $c(P,T,t)$ is deduced. For sufficiently long times t the concentration approaches an equilibrium value c_0, which is used in Sec. III to calculate the net reaction energy. Due to the comparatively long reaction times the accessible range of temperature is restricted, but, as opposed to the measurements of the diffusion parameters, data at one temperature are sufficient to deduce the net reaction energy.

III. EQUILIBRIUM NITROGEN CONCENTRATION

A. Background

The reaction between nitrogen and Sm_2Fe_{17} can be written as

$$\tfrac{1}{2}yN_2(g)+Sm_2Fe_{17}(s)\Leftrightarrow Sm_2Fe_{17}N_y(s). \qquad (2)$$

The equilibrium concentration $c_0=y_0/3$ represents the maximum nitrogen concentration that can be achieved at given temperature T and pressure P.

The solubility of gases in metals is determined by two factors.[10] On one hand, the gas tends to occupy interstitial sites that are energetically favorable. High solubility can be expected if the net reaction energy U_0 of Eq. (2) is negative, so that the binding energy of the interstitial gas atoms in the metal lattice exceeds the molecular binding energy of nitrogen in the gas phase. The binding energy between gas atoms and lattice is mainly due to chemical interaction, but the size of the interstitial site is also important. Small sites require large lattice deformations which require elastic energy. On the other hand, thermal activation tends to create disorder in the gas-solid system. In the extreme high-temperature limit $kT \gg U_0$, this dominates the binding interaction and the solubility approaches an energy-independent value c_∞ when all phase-space configurations have the same probability. An example is the solubility of nitrogen in α-iron which is negligible at low temperatures, because U_0 is positive, but reaches some tenth of an atom percent at high temperatures.[10] The thermal energy of the nitrogen atoms becomes large enough to occupy energetically unfavorable sites.

Nitrogen in R_2Fe_{17} shows a large solubility even at moderately elevated temperatures. At 500 °C and 1 bar nitrogen pressure the majority of all octahedral sites are occupied.[1] This indicates a rather large gas-metal binding energy which is due to the large size of the 9*e* octahedral sites and the distinct chemical affinity between nitrogen and rare-earth atoms which occupy two of the six neighboring lattice sites (Fig. 1). The net reaction energy is negative.

Besides the interaction between gas and metal lattice, the interaction U_1 between different gas atoms in the metal should be considered. This interaction is mainly due to long-range strain fields caused by the lattice deformation around the interstitial atoms.[16] At low temperatures these elastic modes can lead to phase segregation into a gas-poor α phase and a gas-rich β phase. The classic example is palladium hydride below 300 °C which consists of an inhomogeneous two-phase mixture of a hydrogen-poor α phase and a hydrogen-rich β phase, both with the fcc structure of palladium.[10] The critical temperature T_c, below which a two-phase mixture is stable and above which there is a uniform gas-solid solution, depends on U_1.

Downloaded 23 Mar 2007 to 129.93.16.206. Redistribution subject to AIP license or copyright, see http://jap.aip.org/jap/copyright.jsp

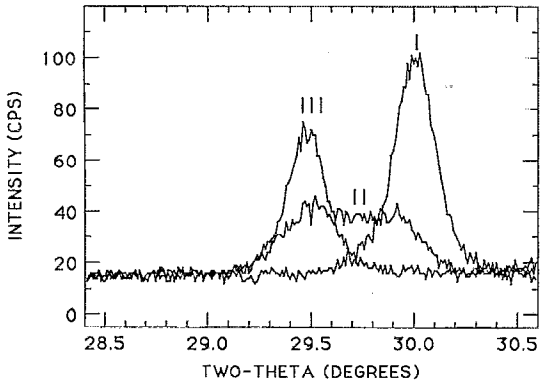

FIG. 2. X-ray-diffraction line shapes for partly nitrogenated ($T=575$ °C) $Sm_2Fe_{17}N_y$ showing the (113) line: I after 0 min; II after 4 min; III after 100 min.

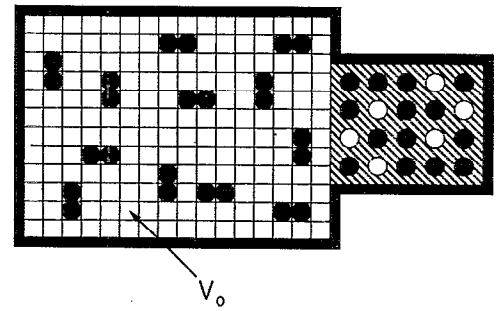

FIG. 3. Schematic illustration of the lattice gas model, showing nitrogen (black circles) in the gas phase (left-hand side) and in solid solution in the intermetallic compound (right-hand side). Note the existence of unoccupied octahedral 9*e* sites (white circles).

At present, the weight of the experimental evidence on $Sm_2Fe_{17}N_y$ at typical nitrogenation temperatures favors a gas-solid solution rather than a two-phase mixture of α-$Sm_2Fe_{17}N_y$ and β-$Sm_2Fe_{17}N_{y'}$. At first the observation of expanded and unexpanded regions in x-ray-diffraction and neutron-diffraction studies suggested a two-phase system.[2,17] However, more recent studies of the annealing behavior of partly nitrided powders and single grains appear to establish that nitrogenation in the temperature range of interest leads to a single phase and intermediate nitrogen content.[18,19]

Further evidence is provided by x-ray line-shape analysis. The data in Fig. 2 immediately show the existence of intermediate lattice parameters which are typically for gas-solid solutions. It is even possible to tune the position of sharp x-ray-diffraction peaks by changing the nitrogen pressure during nitrogenation.[20] Double x-ray- and neutron-diffraction peaks observed in some experiments may be due to incomplete nitrogenation[13] and the radial weighting of the spherical volume element $dV=4\pi r^2\,dr$.

Kerr-effect analysis of partly nitrided grains[18,21] yields another argument in favor of the ideal-solution model. The size of the domains normally increases towards the particle center, because narrow domains become energetically unfavorable with increasing profile depth. However, in the case of $Sm_2Fe_{17}N_y$, the domains become increasingly narrow near the soft core, which indicates a decrease of anisotropy and nitrogen content (see Sec. VI).

Note that the interatomic long-range interaction U_1 depends on the concentration of the interstitial atoms in the lattice.[16] Comparing the nominal compositions PdH and $Sm_2Fe_{17}N_3$ there are more than six times fewer gas atoms per metal atom in the nitride, which might explain the comparatively small influence of the elastic modes.

In the following sections we model the system $Sm_2Fe_{17}N_y$ as an ideal gas-solid solution with U_0 negative and $U_1=0$.

B. Model and results

To calculate the equilibrium properties of the system a lattice-gas model is used. Lattice-gas calculations represent a standard method in statistical physics and presuppose an appropriately simplified phase space.[22]

The model (Fig. 3) consists of a solid with n_s octahedral sites in contact with a large but constant volume of gas V divided into $N_0=V/V_0$ cubic cells. V_0 is the cube of the atomic diameter of molecular nitrogen, about 1 Å^3. μ atoms occupy interstitial sites in the solid while the remainder form $(n-\mu)/2$ nitrogen molecules in the gas phase. The probability for a given microscopic solid-gas configuration Ω is given by

$$P(\Omega)=(1/Z)e^{-\mathbb{H}(\Omega)/kT}, \tag{3}$$

where $\mathbb{H}(\Omega)$ is the energy of the configuration and the partition function Z ensures that the sum of all terms is unity. Neglecting interactions between different nitrogen atoms in the metal, we have

$$\mathbb{H}=\mathbb{H}_0+\tfrac{1}{2}(n-\mu)U_g(N_2)+\mu U_s(N), \tag{4}$$

where $\mathbb{H}_0$ is an arbitrary term that sets the zero of the energy scale, $U_g(N_2)$ is the binding energy per nitrogen molecule, and $U_s(N)$ is the binding energy between a nitrogen atom and the host lattice. Setting $\mathbb{H}_0=-nU_g(N_2)/2$, we obtain $\mathbb{H}=\mu\,U_0$ with U_0, the net reaction energy per nitrogen atom, being defined by

$$U_0=U_s(N)-\tfrac{1}{2}U_g(N_2). \tag{5}$$

Hence,

$$P(\Omega)=(1/Z)e^{-\mu U_0/kT}. \tag{6}$$

Since we are interested in the probability $P_\mu(\mu)$ of finding μ gas atoms in the metal but not in the configuration probability $P(\Omega)$, let $N(\mu)$ be the number of different microscopic states with the same μ. All these states have the same energy $\mathbb{H}=\mu U_0$ and we can write

$$P_\mu(\mu)=(1/Z)N(\mu)e^{-\mu U_0/kT}. \tag{7}$$

Downloaded 23 Mar 2007 to 129.93.16.206. Redistribution subject to AIP license or copyright, see http://jap.aip.org/jap/copyright.jsp

$N(\mu)$ can be determined by simply counting all corresponding states (see the Appendix). In order to find the equilibrium concentration $c_0=\langle\mu\rangle/n_s$ we calculate the thermodynamic mean value

$$\langle\mu\rangle=\sum_{\mu=0}^{n_s}\mu P_\mu(\mu). \tag{8}$$

The summation can be carried out analytically (see the Appendix) and yields the equation of state giving the pressure and temperature dependence of the equilibrium concentration of the gas in the solid:

$$c_0=[1+\sqrt{(3kT/V_0P)}e^{U_0/kT}]^{-1}. \tag{9}$$

Using the abbreviation

$$S_0=\tfrac{1}{2}k\ln(V_0P/3kT), \tag{10}$$

Eq. (9) can be rewritten as

$$[c_0/(1-c_0)]=e^{-(U_0-TS_0)/kT}. \tag{11}$$

Hence $F_0=U_0-TS_0$ is identified as the free-energy difference which determines the equilibrium concentration in the solid. For ideal gases the quantity $c_\infty=\sqrt{V_0P/3kT}$ is small. The value for nitrogen, with $V_0=1$ Å^3, is $c_\infty\sim3\times10^{-3}$, which is comparable to the corresponding experimental value for nitrogen in α-iron.[10] The low-concentration limit

$$c_0=c_\infty e^{-U_0/kT} \tag{12}$$

shows a square-root pressure dependence which is known as Sieverts's law. Note that the solution of nitrogen in α-iron is an endothermic process with $U_0>0$, which ensures low concentrations and the applicability of Eq. (12). The low-pressure variation of Eq. (9), which is the general result, is also $\sqrt{P}$. Fortunately U_0 in Eq. (9) depends only logarithmically on c_0 and c_∞ so reasonable values of U_0 can be determined even if both values of c are imprecisely known.

Note that Eq. (9) refers to a solution process. It must not be confused with superficially similar semiempirical expressions[23] based on van t'Hoff's law which are occasionally used to describe the phase transition between the α and β phases.

The experimentally determined values for the equilibrium content of nitrogen in Sm_2Fe_{17} derived from long-time isothermal absorption analysis are

$$y_0(560\,°\mathrm{C},\ 1.00\ \mathrm{bar})=2.7\pm0.2 \tag{13a}$$

and[20]

$$y_0(500\,°\mathrm{C},\ 0.013\ \mathrm{bar})=1.8\pm0.2, \tag{13b}$$

so we obtain

$$U_0=-57\pm5\ \mathrm{kJ/mol}.$$

Outgassing experiments at $T>700\,°$C confirm this value, but cannot be used to improve its exactness, because disproportionation starts rapidly at these temperatures.

Typical $c_0(T,p)$ curves calculated from Eq. (9) with $U_0=-57$ kJ/mol are shown in Fig. 4. The experimentally accessible zone where equilibrium can be achieved without disproportionation within a reasonable time is shown by the black box. These curves can serve as guide for preparing nitrides of Sm_2Fe_{17} of a desired composition. Quenching from that zone will fix the nitrogen content.

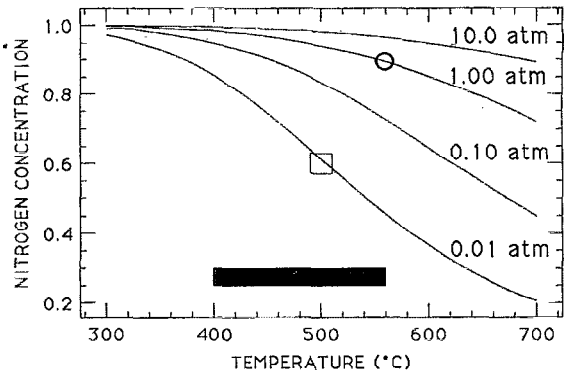

FIG. 4. Equilibrium nitrogen concentrations in Sm_2Fe_{17} as function of temperature and pressure, calculated from Eq. (4) (circle: see Sec. III; square: see Ref. 20). The black bar shows the temperature region where nitrogenation may be carried out.

IV. DIFFUSION OF NITROGEN IN $Sm_2Fe_{17}N_y$

A. Diffusion constant and nitrogen profiles

At typical nitrogenation temperatures the gas-solid reaction proceeds by thermally activated bulk diffusion within the particles. At lower temperatures (below about 350 °C) surface effects have to be taken into account. Neglecting any anisotropic diffusion the nitrogen profiles are found by solving the diffusion equation

$$\frac{\partial c}{\partial t}=D\nabla^2c, \tag{14}$$

subject to the boundary condition $c(\mathbf{r}_s,t)=c_0$ at the particle surface. We continue to restrict ourselves to the case with no interatomic interaction. Then the chemical diffusion constant D is independent of the concentration[24] and Eq. (14) represents a linear differential equation. In the case of spherical particles of radius R the boundary value problem Eq. (14) can be solved analytically:[11]

$$c(r,t)=c_0\left(1+\frac{2R}{\pi r}\sum_{m=1}^{\infty}(-1)^m\frac{1}{m}\sin\frac{m\pi r}{R}e^{-m^2\pi^2Dt/R^2}\right). \tag{15}$$

Volume integration of Eq. (15) yields

$$\langle c\rangle=c_0\left(1-\frac{6}{\pi^2}\sum_{m=1}^{\infty}\frac{1}{m^2}e^{-m^2\pi^2Dt/R^2}\right). \tag{16}$$

Note that c_0 is given by Eq. (9) and merely acts as a prefactor. Some typical nitrogen profiles are shown in Fig. 5. Equation (15) can be used to calculate x-ray- and neutron-diffraction line profiles if we assume that the line intensity is proportional to the volume fraction of the material with the corresponding lattice expansion.[25] The calculated line shape for spherical grains with $c_0=0.37$ ($y=1.1$) is presented in Fig. 6.

Downloaded 23 Mar 2007 to 129.93.16.206. Redistribution subject to AIP license or copyright, see http://jap.aip.org/jap/copyright.jsp

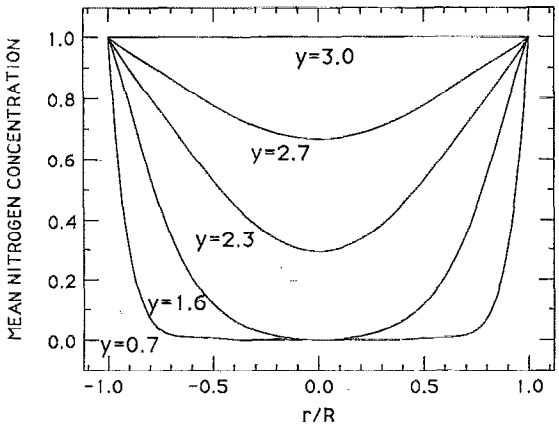

FIG. 5. Nitrogen concentration profiles for spherical particles. The equilibrium nitrogen content is taken as 3.0.

Obviously, weighting by the spherical volume element $4\pi r^2\, dr$ in the integration can lead to a double-peak line shape even when diffusion profiles are smooth as in Fig. 5. Double-peak diffraction lines are not a sufficient condition to infer the existence of two phases α-$Sm_2Fe_{17}N_y$ and β-$Sm_2Fe_{17}N_{y'}$ (see Sec. III A and Ref. 13).

Note that apparently well-nitrogenated grains $Sm_2Fe_{17}N_{2.3}$ consists of a shell with $y \approx 3$ and small core with $y \approx 1$ only.

B. Dependence on shape and size distribution

The calculations of nitrogen profiles for nonspherical particles is more difficult; but, so long as there is no overlay of different diffusion fronts, curves with positive curvature similar to those of Fig. 5 must always be expected. In no case does Eq. (14) yield a sharp transition between nitrogen-rich and nitrogen-poor regions that would resemble epitaxial growth. This is due to the fact that any sharp-edged diffusion front has regions with locally negative curvature $\nabla^2 c < 0$. This yields a local concentration decrease during the nitrogenation process, which is physically unreasonable.

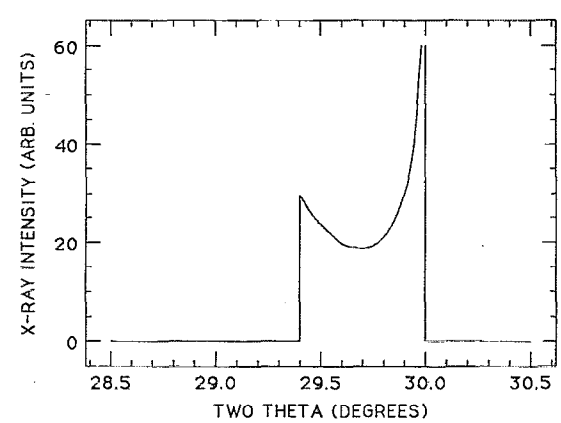

FIG. 6. Calculated (113) x-ray line shape for $Sm_2Fe_{17}N_{1.1}$, neglecting the natural line broadening. The left-hand-side low-angle peak corresponds to the nitrogenated region near the surface whereas the right-hand-side one is due to the un-nitrogenated core.

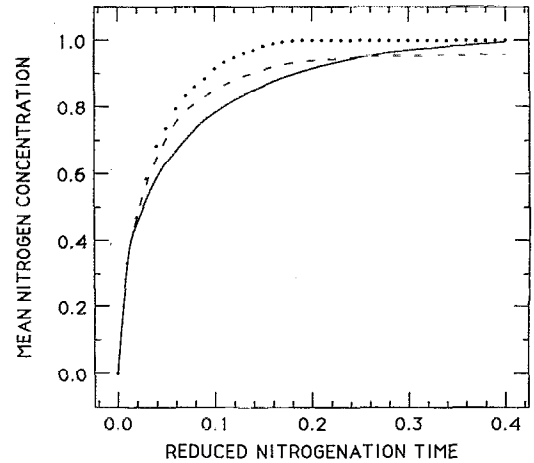

FIG. 7. Dependence of the mean nitrogen concentration in particles with different shapes on the reduced nitrogenation time Eq. (17). Solid line: spherical particles with no size distribution; dashed line: spherical particles with the size distribution Eq. (20); dotted line: thin plates with no size distribution.

Besides particle shape, the particle size plays an important role. The time necessary for nitrogenation scales as R^2, hence large particles remain partly nitrogenated even after long nitrogenation times. In order to simplify the analysis it is appropriate to define a reduced nitrogenation time τ,

$$\tau = DA_p^2 t / 9V_p^2, \tag{17}$$

where A_p is the total powder surface area and V_p the total powder volume. For spherical grains of uniform size we have

$$\tau = Dt/R^2. \tag{18}$$

Note that τ is the essential parameter in Eqs. (15) and (16). Figure 7 shows the mean concentration $\langle c \rangle$ as function of τ for different powders. In the initial stage the rate of the gas-solid reaction is simply proportional to the total powder surface area and the mean concentration is given by the universal formula

$$\langle c \rangle = 6c_0 \sqrt{\tau/\pi}. \tag{19}$$

The long-time behavior depends on the particle shape and size distribution. The case of thin plates illustrates how changes in the particle shape influence the diffusion behavior.[11] Nonspherical particles lead to shorter nitrogenation times for a given specific surface area A_p/V_p, because the sphere is the particle with the smallest specific surface.

Particle size distributions lead to an initially swift nitrogenation which goes over into a very slow approach to saturation. This long-time tail is exponential for monodisperse powders but power-law-like for polydisperse ensembles. To calculate the dashed curve in Fig. 7 the size distribution

Downloaded 23 Mar 2007 to 129.93.16.206. Redistribution subject to AIP license or copyright, see http://jap.aip.org/jap/copyright.jsp

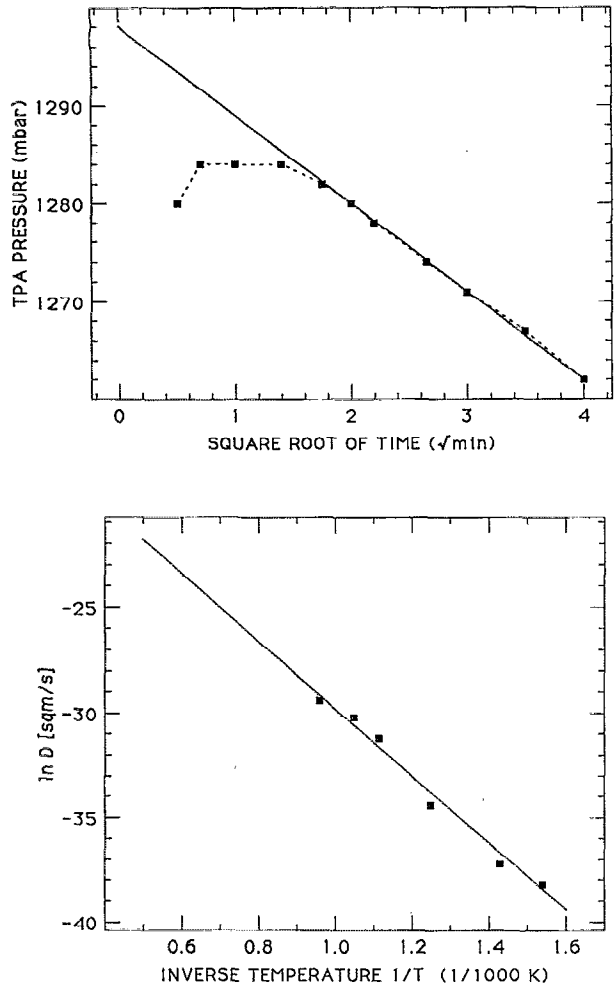

FIG. 8. (a) A typical short-time TPA nitrogenation curve for $Sm_2Fe_{17}N_y$ at $T=425$ °C. (b) Arrhenius plot for $D(T)$ derived from data as in (a).

$$P(R)=\frac{5R_0^5}{R^6}\Theta(R-R_0) \tag{20}$$

was used, which gives a $1/t$ long-time dependence of $\langle c\rangle$. $\Theta(x)=1$ for $x>0$ and 0 for $x<0$.

C. Experimental determination of the diffusion constants

Since the short-term absorption of nitrogen is actually independent of particle shape, we have used short-time thermopiezic analysis (TPA) measurements to determine E_a and D_0. According to Eq. (19) the mean nitrogen content and hence the change in nitrogen pressure should be proportional to $\sqrt{t}$. Figure 8(a) shows a typical square-root plot ($T=425$ °C).

The Arrhenius plot Fig. 8(b) includes six temperatures between 375 and 775 °C (see Sec. II) and yields an activation energy of 133 ± 5 kJ/mol. The magnitude of D_0 is 1.02 mm^2/s. Both values can be regarded as typical for nitrogen in metals.[10,11] Note that D_0 values significantly smaller than 1 mm^2/s correspond to a negative activation entropy, which is physically unreasonable in the present context.

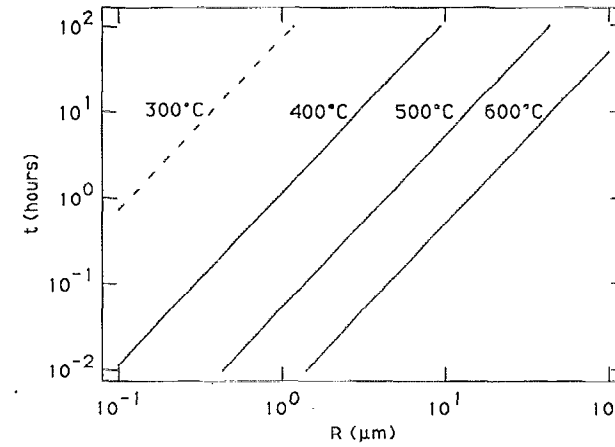

FIG. 9. Approximate nitrogenation time for spherical grains as function of particle radius R and temperature.

Finally, we plot in Fig. 9 the time that is necessary to produce reasonably well-nitrogenated spherical grains at different temperatures ($\langle c\rangle=0.90c_0$). More exact results may be obtained using Fig. 7.

V. STRESS AND STRAIN

A. Calculation

Inhomogeneous nitrogen profiles cause inhomogeneous mechanical stress and strain. The nitrogenated outer shell cannot expand freely because it is connected to the un-nitrogenated core. Here we calculate the elastic stress and strain profiles for given nitrogen profiles. Our approach neglects secondary modifications of the nitrogen profiles due to interaction effects and incoherent states due to plastic deformation.[16] Assuming a linear relation between lattice expansion and nitrogen content, the expansion of a homogeneously nitrogenated grain is given by

$$\epsilon_{ij}^H=\langle c\rangle\epsilon_0\delta_{ij}\,. \tag{21}$$

The volume expansion $\epsilon_V^H=\mathrm{Tr}\,\epsilon_{ij}^H$; therefore,

$$\epsilon_V^H=3\langle c\rangle\epsilon_0\,. \tag{22}$$

Hence, the maximum volume expansion of about 6% corresponds to $\epsilon_0=0.02$.[1,2]

In inhomogeneously nitrogenated grains, ϵ_{ij}^H can be defined as a local quantity depending on nitrogen concentration,

$$\epsilon_{ij}^H(\mathbf{r})=c(\mathbf{r})\epsilon_0\delta_{ij}\,, \tag{23}$$

but the local expansion $\epsilon_{ij}(\mathbf{r})$ is now no longer just given by ϵ_{ij}^H. To calculate ϵ_{ij} we use the model of an elastically isotropic crystal. The difference $\delta_{ij}-\epsilon_{ij}^H$ is assumed to be sufficiently small so that the system obeys Hooke's law,

$$\sigma_{ij}=\frac{E}{1+v}(\epsilon_{ij}-\epsilon_{ij}^H)+\frac{\nu E}{(1+\nu)(1-2\nu)}\delta_{ij}\,\mathrm{Tr}(\epsilon_{ij}-\epsilon_{ij}^H)\,. \tag{24}$$

Downloaded 23 Mar 2007 to 129.93.16.206. Redistribution subject to AIP license or copyright, see http://jap.aip.org/jap/copyright.jsp

Young's modulus E and Poisson's ratio ν are assumed to be concentration independent; σ_{ij} is the stress tensor. The solution minimizes the elastic energy U_E of the free grain:[26]

$$U_E=\frac{1}{2}\sum_{i,j=1}^{3}\int(\epsilon_{ij}-\epsilon_{ij}^{H})\sigma_{ij}\,dV. \tag{25}$$

In the case of spherical particles ϵ_{ij} can be represented as

$$\epsilon_{ij}(\mathbf{r})=\int_0^R G_{ij}^{\epsilon}(\mathbf{r},r')c(r')dr', \tag{26}$$

where R is the particle radius and G_{ij}^{ϵ} is the elastic Green's function of the problem. Note that Eq. (26) allows the immediate calculation of $\epsilon_{ij}(\mathbf{r})$ for arbitrary concentration profiles. In Eq. (26) the local concentration $c(r)$ acts as an inhomogeneity which causes the strain $\epsilon_{ij}(\mathbf{r})$ via G_{ij}^{ϵ}. The corresponding values $\sigma_{ij}(\mathbf{r})$ can easily be calculated using Eq. (24).

To determine G_{ij}^{ϵ} we have to take into account the spherical symmetry of the problem. Together with the continuity of the deformation, this condition yields the following diagonal Cartesian representation of ϵ_{ij}:[26]

$$\epsilon_{ij}=\begin{pmatrix}\epsilon_r & 0 & 0\\ 0 & \epsilon_1 & 0\\ 0 & 0 & \epsilon_1\end{pmatrix}, \tag{27}$$

with the radial strain

$$\epsilon_r=\varphi(r)+r\frac{d\varphi}{dr}(r), \tag{28}$$

and the lateral strain parallel to the surface

$$\epsilon_1=\varphi(r). \tag{29}$$

Minimization of U_E with respect to the unknown function $\varphi(r)$ yields G_{ij}^{ϵ} in diagonal representation,[26]

$$G_{ij}^{\epsilon}=\begin{pmatrix}G_r^{\epsilon}(r,r') & 0 & 0\\ 0 & G_1^{\epsilon}(r,r') & 0\\ 0 & 0 & G_1^{\epsilon}(r,r')\end{pmatrix}, \tag{30}$$

with

$$G_1^{\epsilon}(r,r')=\epsilon_0 r'^2\left(\frac{2(1-2\nu)}{(1-\nu)R^3}+\frac{1+\nu}{(1-\nu)r^3}\Theta(r-r')\right) \tag{31}$$

and

$$G_r^{\epsilon}(r,r')=G_1^{\epsilon}(r,r')+r\frac{\partial}{\partial r}G_1^{\epsilon}(r,r'). \tag{32}$$

Due to the simple structure of these equations, the integration of Eq. (26) can be carried out explicitly and we obtain the solutions

$$\epsilon_1(r)=\epsilon_0\left(\langle c\rangle+\frac{1+\nu}{3(1-\nu)}[c_M(r)-\langle c\rangle]\right) \tag{33a}$$

and

$$\epsilon_r(r)=\epsilon_0\left(\langle c\rangle+\frac{1+\nu}{3(1-\nu)}[3c(r)-2c_M(r)-\langle c\rangle]\right). \tag{33b}$$

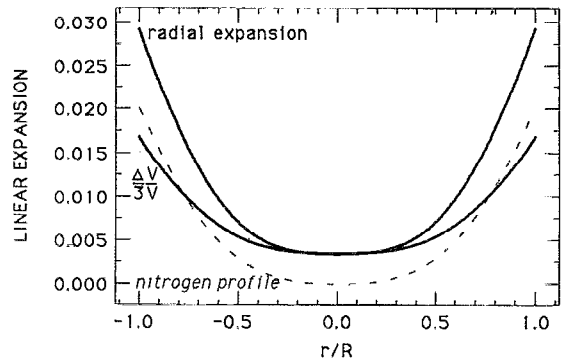

FIG. 10. Radial and volume expansion for a spherical grain $Sm_2Fe_{17}N_{1.6}$.

$c_M(r)$ is an auxiliary mean value function,

$$c_M(r)=\frac{3}{r^3}\int_0^r c(\xi)\xi^2\,d\xi \tag{34}$$

which represents the mean nitrogen concentration of a spherical core with the radius r so that $c_M(0)=c(0)$ and $c_M(R)=\langle c\rangle$. The local volume expansion $\epsilon_V=\mathrm{Tr}\,\epsilon_{ij}$ is

$$\epsilon_V(r)=\epsilon_0\left(3\langle c\rangle+\frac{1+\nu}{1-\nu}[c(r)-\langle c\rangle]\right). \tag{35}$$

Note that the local nitrogen concentration $c(r)$ and the mean nitrogen concentration of the whole grain are sufficient to determine $\epsilon_V(r)$.

Figure 10 shows the functions $\epsilon_r(r)$ and $\epsilon_V(r)$ for a spherical particle $Sm_2Fe_{17}N_{1.6}$. Two striking results are (i) the expansion of the core even in the absence of any nitrogen there, and (ii) the large radial strain near the surface which exceeds ϵ_0 by about 50%. Both phenomena are discussed in more detail in Sec. VI.

The total elastic energy due to the inhomogeneous nitrogen profile is

$$U_E=[4\pi ER^3/3(1-\nu)]\epsilon_0^2(\langle c^2\rangle-\langle c\rangle^2). \tag{36}$$

Assuming $E=150$ GPa and $\nu=\frac{1}{3}$ we get an energy of less than 3 kJ per mole of nitrogen atoms, a magnitude small in comparison with the net reaction energy of -57 kJ/mol. Note that this value does not include the energy that is necessary to expand the lattice around the 9e sites. This energy contributes to U_0 and is independent of the macroscopic deformation state.

As can be seen from Fig. 10, the radial expansion near the surface considerably exceeds the value ϵ_0 of the fully nitrogenated grain. The constraint produces a lateral compression which leads via Poisson's ratio to the large radial expansion. At $r=R$ we find from Eq. (33b)

$$\epsilon_r(R)-\epsilon_0=2\nu\epsilon_0(c_0-\langle c\rangle). \tag{37}$$

The time dependence of $\epsilon_r(R)$ is shown in Fig. 11. Obviously the effect is largest in the initial stages of nitrogenation.

Downloaded 23 Mar 2007 to 129.93.16.206. Redistribution subject to AIP license or copyright, see http://jap.aip.org/jap/copyright.jsp

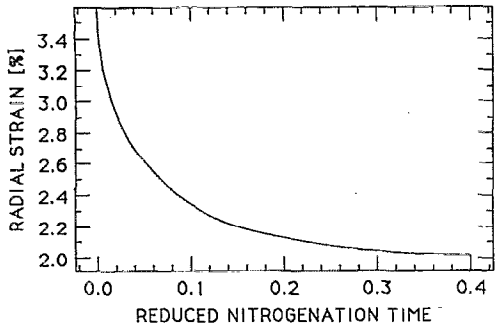

FIG. 11. Dependence of the excess strain on the reduced nitrogenation time Eq. (17) for spherical grains.

B. X-ray analysis

X-ray diffraction in the θ-2θ geometry weights diffraction from planes parallel to and near the surface, hence we should expect to see this excess strain in the surface region of the particles by x rays. Starting with x-ray line profiles like those in Fig. 2 and using the Siemens DIFF program the (113) reflection was represented as overlay of lines with fixed width.

The $\langle c \rangle$ dependence of the low-angle component is shown in Fig. 12. The curve qualitatively agrees with Eq. (37) but the error bars indicate the need for a more sophisticated analytical procedure. Note that Eq. (16) and Fig. 12 yield the rather small value $\nu=0.21$, which could reflect the onset of plastic deformation.

VI. EFFECTS ON PROCESSING AND MAGNETIC PROPERTIES

A. Excess strain

The strongly uniaxial deformation near the surface may be important with respect to the disproportionation of $Sm_2Fe_{17}N_y$ into α-iron and SmN which destroys coercivity. Experience shows that most free iron is produced in the initial stages of nitrogenation.[5] X-ray diffraction of reground powders, Mössbauer conversion electron measurements, and the fact that metal bonding remarkably improves the coercivity all indicate that α-iron is deposited preferentially at the particles' surface.[27,28] The possible cause is excess strain near the surface which intensifies the instability of the metastable $Sm_2Fe_{17}N_y$ phase by promoting irreversible processes such as diffusion of α-iron and samarium in the 2:17 lattice. Note that $\epsilon_r(R)-\epsilon_0$ is predicted to exceed 1%, the limit of validity of Hooke's law in metals, and there could be plastic changes of the lattice structure.

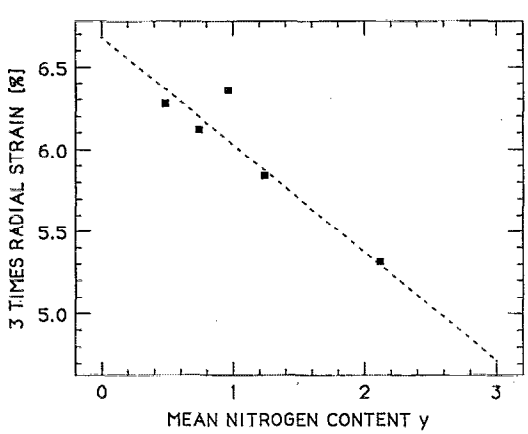

FIG. 12. The low-angle component of the (113) x-ray-diffraction peak as function of the mean nitrogen content, derived from data like those in Fig. 2.

Possible ways to avoid this surface disproportionation are to begin the nitrogenation at a sufficiently low temperature[19] or else to pre-expand the lattice using hydrogen, and then displace the hydrogen by nitrogen. Hydrogen decrepitation is also a possible way of improving the processing properties by reducing the effective particle radius R. Grain boundary diffusion will have a similar effect.

B. Curie temperature

The Curie temperature increase of R_2Fe_{17} nitrides is mainly due to the volume expansion of the lattice (see Sec. I). In homogeneously nitrogenated grains the lattice expansion can be interpreted as dependent on the local nitrogen concentration; however, in the inhomogeneous case this dependence is modified by the macroscopic strain. Figure 10 shows strain and nitrogen profiles of a partly nitrogenated grain with practically no nitrogen at the center, but significant lattice expansion $\Delta V/V=1.1\%$. This core expansion is described by Eq. (35). In the initial stage we have $c(0)=0$ and

$$\epsilon_V(0)=[2(1-\nu)/(1-\nu)]\epsilon_0\langle c\rangle. \tag{38}$$

Incompressible materials have $\nu=\frac{1}{2}$ and show no core expansion.

Assuming a linear dependence of the Curie temperature on ϵ_V, Fig. 13(a) gives the Curie temperature of the core of the particle at $r=0$ as function of y. Note that the mean volume expansion

$$\langle \epsilon_V\rangle=3\epsilon_0\langle c\rangle \tag{39}$$

is identical with the homogeneous case. Hence, the core expansion merely leads to a homogenization of the volume expansion without shifting the mean value $\langle \epsilon_V\rangle$. However, due to the relation

$$\frac{\partial^2 M_s}{\partial T_c^2}<0, \tag{40}$$

a shift of M_s can be expected. For instance, milling of partly nitrogenated particles will release the stress and produce a certain decrease of the average saturation magnetization.

An important consequence of the core expansion is the existence of regions with elevated Curie temperature but negative anisotropy K_1, the "soft center" problem.

C. Anisotropy and coercivity

The maximum coercivity of a particle depends on the anisotropy constant K_1. For pure Sm_2Fe_{17}, K_1 is negative

Downloaded 23 Mar 2007 to 129.93.16.206. Redistribution subject to AIP license or copyright, see http://jap.aip.org/jap/copyright.jsp

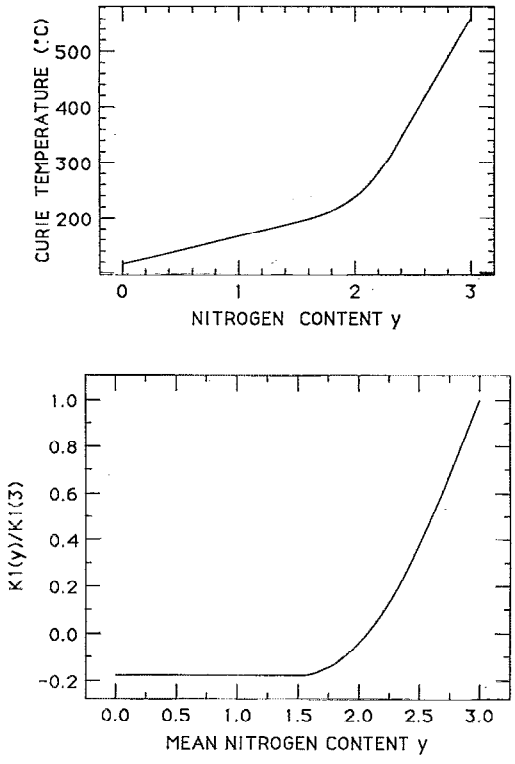

FIG. 13. (a) The concentration dependence of the Curie temperature at the center of a spherical particle. (b) The concentration dependence of the anisotropy constant K_1 at the center of a spherical particle, as a function of average nitrogen content.

(easy plane) but as nitrogen enters the $9e$ sites it creates a strong electric-field gradient at the Sm $4f$ shell. The crystal-field coefficients such as A_{20} in particular are modified and K_1 increases.[8] The grain center is a critical region, because so long as K_1 remains negative there it will act as a nucleation center for reverse domains, and hence destroy coercivity. The dependence of $K_1(0)$ on y is given in Fig. 13(b). Only particles with $y>2.1$ can be expected to yield any appreciable coercivity.

One solution to the soft center problem is to remill the powder after nitrogenation, which isolates the center as a separate fine grain and allows the remaining fragments of the outer, magnetically hard region to develop coercivity.

VII. CONCLUSIONS

From a treatment of the statistical mechanics of the gas-phase interstitial nitrogenation reaction Eq. (2) which neglects interactions between different interstitial atoms, we have obtained the equation of state Eq. (9) for the equilibrium nitrogen concentration as a function of pressure and temperature. The model is applied to $Sm_2Fe_{17}N_y$, which appears to behave as a gas-solid solution in the accessible temperature range, rather than a two-phase system. Curves showing the equilibrium nitrogen content as a function of pressure and temperature have been generated (Fig. 4), and the net reaction energy U_0 is derived as -57 ± 5 kJ/mol. The model can be refined, if necessary, to take into account interatomic interaction U_1 in the nitride, and calculate the properties of the two-phase region at low temperatures.

Nitrogen diffusion in Sm_2Fe_{17} has been reexamined, and values of D_0 and E_a are derived from the $\sqrt{t}$ variation in the initial stage of nitrogenation where the behavior is independent of particle shape. The values $D_0=1.02$ mm^2/s and $E_a=133$ kJ/mol are typical for nitrogen in metals and have been used to calculate nitrogen concentration profiles and $\langle c(T)\rangle$ curves.

Stress and strain in inhomogeneously nitrogenated grains have been investigated in the linear elastic approximation. The calculated stress and strain profiles show an expanded particle center even in the initial stages. Large uniaxial strain near the particle surface is predicted and there is a likely influence of this excess strain on the disproportionation of the nitride and its coercivity.

In the initial stage of nitrogenation, stress and strain lead to an expanded particle center with increased Curie temperature but negative K_1. This "soft center," which is found in particles with average nitrogen contents as high as $y=2.1$, is likely to act as a nucleation center and to destroy coercivity.

ACKNOWLEDGMENTS

We are grateful to H. Sun and S. Wirth for help with part of this work. This work forms part of the "Concerted European Action on Magnets." It was supported by the BRITE/EURAM Programme of the European Commission.

APPENDIX

To determine $\langle\mu\rangle=n_s c_0$ we have to calculate the partition function

$$Z=\sum_{\mu=0}^{n_s} N(\mu)e^{-\mu U_0/kT} \tag{A1}$$

of the model system. $N(\mu)$ consists of three independent factors:

$$N(\mu)=N_G(\mu)N_C(\mu)N_S(\mu). \tag{A2}$$

N_G is the number of different gas configurations of the $n-\mu$ nitrogen atoms. The first atom can occupy N_0 different states. The second atom is connected with the first one, hence it must occupy one of the six neighboring sites. The third atom finds N_0-2 free sites and so on. Assuming an ideal gas with $n\ll N_0$ we can neglect double occupation, i.e., all atoms with even numbers can occupy N_0 states, all atoms with odd numbers six neighboring sites. Taking into account the permutability of the atoms in a molecule, which yields $3=6/2$ orientations per molecule, we obtain

$$N_G(\mu)=N_0^{(n-\mu)/2}3^{(n-\mu)/2}. \tag{A3}$$

$N_C(\mu)$ is the number of different ways to choose $\mu/2$ molecules. Since $n_s\ll n$ (sufficiently small sample mass) we have

$$N_C(\mu)=(n/2)^{\mu/2}. \tag{A4}$$

Downloaded 23 Mar 2007 to 129.93.16.206. Redistribution subject to AIP license or copyright, see http://jap.aip.org/jap/copyright.jsp

The $\mu/2$ molecules dissociate and must be distributed over the n_s interstitial sites. Usually μ reaches the same order of magnitude as n_s and approximations as for $N_G(\mu)$ and $N_C(\mu)$ are not possible. Taking into account that each site can be occupied by one gas atom only (the site blocking assumption of lattice gas statistics) we obtain

$$N_s(n)=n_s/[(n_s-\mu)!\mu!]. \tag{A5}$$

Hence

$$Z=(6N_0)^{n/2}\sum_{\mu=0}^{n_s}\frac{n_s!}{(n_s-\mu)!\mu!}\left(\frac{n}{6N_0}\right)^{\mu/2}e^{-\mu U_0/kT}. \tag{A6}$$

Using the binomial expression

$$(a+b)^m=\sum_{k=0}^{m}\frac{m!}{(m-k)!k!}a^{m-k}b^k, \tag{A7}$$

we obtain with $a=1$

$$Z=(6N_0)^{n/2}(1+\sqrt{(n/6N_0)}e^{-\mu U_0/kT})^{n_s}. \tag{A8}$$

As expected for systems without interaction between different atoms in the lattice, Z is essentially a product of n_s independent terms. The equilibrium mean value of μ is given by

$$\langle\mu\rangle=\frac{1}{Z}\sum_{\mu=0}^{n_s}\mu N(\mu)e^{-\mu U_0/kT}. \tag{A9}$$

Using the derivative

$$\frac{\partial Z}{\partial U_0}=-\frac{1}{kT}\sum_{\mu=0}^{n_s}\mu N(\mu)e^{-\mu U_0/kT} \tag{A10}$$

yields

$$\langle\mu\rangle=-kT\frac{1}{Z}\frac{\partial Z}{\partial U_0} \tag{A11}$$

and

$$\langle\mu\rangle=\frac{n_s}{1+\sqrt{(n/6N_0)}e^{\mu U_0/kT}}. \tag{A12}$$

With $V=N_0V_0$, $PV=(n/2)kT$, and $\langle\mu\rangle n_s c_0$ we get the final result, Eq. (9). Note that the ratio T/P in Eq. (9) does not depend on T.

[1] J. M. D. Coey and H. Sun, J. Magn. Magn. Mater. **87**, L251 (1990); H. Sun, J. M. D. Coey, Y. Otani, and D. P. F. Hurley, J. Phys. Condensed Matter **2**, 6465 (1990).

[2] J. M. D. Coey, J. F. Lawler, H. Sun, and J. E. M. Allan, J. Appl. Phys. **69**, 3007 (1991).

[3] T. W. Capchart, R. K. Mishra, and F. E. Pinkerton, Appl. Phys. Lett. **58**, 1395 (1991).

[4] B.-P. Hu, H.-S. Li, H. Sun, J. F. Lawler, and J. M. D. Coey, Solid State Commun. **76**, 587 (1990).

[5] M. Katter, J. Wecker, L. Schultz, and R. Grössinger, J. Magn. Magn. Mater. **92**, L14 (1990).

[6] K. Schnitzke, L. Schultz, J. Wecker, and M. Katter, Appl. Phys. Lett. **57**, 2853 (1990).

[7] K. H. J. Buschow, R. Coehoorn, D. B. de Mooij, K. de Waard, and T. H. Jacobs, J. Magn. Magn. Mater. **92**, L35 (1990).

[8] J. M. D. Coey, Phys. Scr. **T39**, 21 (1991); J. M. D. Coey, H. Sun, and D. P. F. Hurley, J. Magn. Magn. Mater. **103**, 310 (1991).

[9] O. Isnard, S. Miraglia, J. L. Soubeyroux, J. Pannetier, and D. Fruchart, Phys. Rev. B **45**, 2920 (1992).

[10] J. D. Fast, *Gases in Metals* (Macmillan, London, 1976).

[11] B. S. Bochstein, *Diffusion in Metals* (in Russian) (Metallurgija, Moscow, 1978).

[12] S. S. Jaswal, W. B. Yelon, G. C. Hadjipanayis, Y. Z. Yang, and D. J. Sellmyer, Phys. Rev. Lett. **67**, 644 (1991).

[13] Well-defined powder fractions are a necessary precondition to study the gas-phase interstitial modification reaction. Nitrogenation of unsieved powder yields a mixture of fully nitrogenated small particles and nearly unnitrided large particles, which may mimic a two-phase system.

[14] Measurements performed at a rapid heating rate are unsuitable for investigating the gas-solid reaction, because U_0 refers to equilibrium states only. At a heating rate of order 10 deg per minute, it is possible only to investigate reactions that occur within a few minutes, whereas the nitrogenation reaction may take hours. In fact, differential scanning calorimetry measurements show endothermic peaks for the Sm_2Fe_{17}-N_2 reaction (Ref. 15) although the nitrogen density in $Sm_2Fe_{17}N_3$ is much larger than in the gas phase, so the reaction has to be exothermic to compensate for the loss in entropy. The endotherms reflect the initial stage of the reaction, probably the desorption of adsorbed gas molecules and the dissociation of the nitrogen molecules.

[15] M. Katter, thesis, Technische Universität Wien, 1992.

[16] H. Wagner and H. Horner, Adv. Phys. **23**, 587 (1974).

[17] O. Isnard, J. L. Soubeyroux, S. Miraglia, D. Fruchart, L. M. Garcia, and J. Bartholome, Physica B (to be published).

[18] T. Mukai and T. Fujimoto, J. Magn. Magn. Mater. **103**, 165 (1992).

[19] M. Katter, J. Wecker, C. Kuhrt, L. Schultz, and R. Grössinger, J. Magn. Magn. Mater. **117**, 419 (1992).

[20] J. M. D. Coey, R. Skomski, and S. Wirth, IEEE Trans. Magn. **MAG-28**, 2332 (1992).

[21] K.-H. Müller, P. A. P. Wendhausen, D. Eckert, and A. Handstein, in Proceedings of the 7th International Symposium on Magnetic Anisotropy and Coercivity in RE-TM Alloys, Canberra, Australia, July 1992, p. 34.

[22] T. D. Lee and C. N. Yang, Phys. Rev. **87**, 410 (1952).

[23] R. M. Ibberson, O. Moze, T. H. Jacobs, and K. H. J. Buschow, J. Phys. Condensed Matter **3**, 1219 (1991).

[24] R. Kuttner, K. Binder, and K. W. Kehr, Phys. Rev. B **26**, 2967 (1982).

[25] In the case of x rays, there is an additional modification due to absorption.

[26] R. Skomski (unpublished).

[27] Y. Otani, D. P. F. Hurley, H. Sun, and J. M. D. Coey, J. Appl. Phys. **69**, 6735 (1991).

[28] T. Bakas (unpublished).

Downloaded 23 Mar 2007 to 129.93.16.206. Redistribution subject to AIP license or copyright, see http://jap.aip.org/jap/copyright.jsp